• Basic Research •

Abnormal function of *EPHA2*/p.R957P mutant in congenital cataract

Jing-Jin Zhang[1,2], *Zong-Fu Cao*[3,4], *Bi-Ting Zhou*[1,2], *Ju-Hua Yang*[1,2,5], *Zhong Li*[5], *Shuang Lin*[5], *Xiao-Le Chen*[5], *Nan-Wen Zhang*[5], *Qin Ye*[1,2], *Xu Ma*[3,4], *Yi-Hua Zhu*[1,2]

[1]Department of Ophthalmology, the First Affiliated Hospital of Fujian Medical University; Fujian Institute of Ophthalmology; Fujian Provincial Clinical Medical Research Center of Eye Diseases and Optometry, Fuzhou 350005, Fujian Province, China
[2]Department of Ophthalmology, National Regional Medical Center, Binhai Campus of the First Affiliated Hospital, Fujian Medical University, Fuzhou 350005, Fujian Province, China
[3]Chinese Academy of Medical Sciences & Peking Union Medical College, Beijing 100000, China
[4]National Human Genetic Resources Center, National Research Institute for Family Planning, Beijing 100081, China
[5]Department of Bioengineering and Biopharmaceutics, School of Pharmacy, Fujian Medical University, Fuzhou 350004, Fujian Province, China
Co-first authors: Jing-Jin Zhang, Zong-Fu Cao, and Bi-Ting Zhou
Correspondence to: Qin Ye. The First Affiliated Hospital of Fujian Medical University, No.20, Chazhong Road, Fuzhou 350005, Fujian Province, China. ophyq810814@163.com; Xu Ma. National Human Genetic Resources Center, National Research Institute for Family Planning, Beijing 100081, China. maxubioinfo@163.com; Yi-Hua Zhu. Department of Ophthalmology, the First Affiliated Hospital of Fujian Medical University, No.20, Chazhong Road, Fuzhou 350005, Fujian Province, China. zhuyihua209@163.com
Received: 2023-12-07 Accepted: 2024-03-18

Abstract

● **AIM:** To identify genetic defects in a Chinese family with congenital posterior polar cataracts and assess the pathogenicity.

● **METHODS:** A four-generation Chinese family affected with autosomal dominant congenital cataract was recruited. Nineteen individuals took part in this study including 5 affected and 14 unaffected individuals. Sanger sequencing targeted hot-spot regions of 27 congenital cataract-causing genes for variant discovery. The pathogenicity of the variant was evaluated by the guidelines of American College of Medical Genetics and InterVar software. Confocal microscopy was applied to detect the subcellular localization of fluorescence-labeled ephrin type-A receptor 2 (EPHA2). Co-immunoprecipitation assay was implemented to estimate the interaction between EphA2 and other lens membrane proteins. The mRNA and protein expression were analyzed by reverse transcription-polymerase chain reaction (qRT-PCR) and Western blotting assay, respectively. The cell migration was analyzed by wound healing assay. Zebrafish model was generated by ectopic expression of human *EPHA2*/p.R957P mutant to demonstrate whether the mutant could cause lens opacity *in vivo*.

● **RESULTS:** A novel missense and pathogenic variant c.2870G>C was identified in the sterile alpha motif (SAM) domain of *EPHA2*. Functional studies demonstrated the variant's impact: reduced EPHA2 protein expression, altered subcellular localization, and disrupted interactions with other lens membrane proteins. This mutant notably enhanced human lens epithelial cell migration, and induced a central cloudy region and roughness in zebrafish lenses with ectopic expression of human *EPHA2*/p.R957P mutant under differential interference contrast (DIC) optics.

● **CONCLUSION:** Novel pathogenic c.2870G>C variant of *EPHA2* in a Chinese congenital cataract family contributes to disease pathogenesis.

● **KEYWORDS:** congenital cataract; *EPHA2*; missense variant; function analysis

DOI:10.18240/ijo.2024.06.04

Citation: Zhang JJ, Cao ZF, Zhou BT, Yang JH, Li Z, Lin S, Chen XL, Zhang NW, Ye Q, Ma X, Zhu YH. Abnormal function of *EPHA2*/p.R957P mutant in congenital cataract. *Int J Ophthalmol* 2024;17(6):1007-1017

INTRODUCTION

Congenital cataract (CC) is a prevalent cause of childhood blindness. The incidence ranges from 2.2 to 13.6 cases per 10 000 children globally, with Asia having the highest prevalence at 7.43 per 10 000[1]. While timely surgery can help preserve vision, predicting outcomes remains challenging[2]. The pathogenesis of CC is complex, involving factors like

heredity, infections, metabolism issues, X-ray exposure, drugs, and more. Heredity contributes significantly, accounting for 30% of cases, often through autosomal dominant inheritance[3]. Currently, over seventy pathogenic loci linked to CC have been identified, categorized by function, such as crystalline, cytoskeleton-related, membrane, and growth factor genes[4-5].

Ephrin type-A receptor 2 (EPHA2, OMIM:176946) is a prominent member of the ephrin (Eph) receptor tyrosine kinase family, playing a pivotal role in essential cellular functions such as differentiation, migration, intercellular adhesion, and tissue morphogenesis[6-7]. Initially termed epithelial cell kinase (eck), the protein encoded by *EPHA2* holds a widespread presence among epithelial cell populations. The EPHA2 receptor is a 130-kDa transmembrane glycoprotein consisting of 976 amino acids[8]. Its structure comprises extracellular (N-terminal), transmembrane, and intracellular (C-terminal) segments. The extracellular region includes an ephrin ligand binding domain (LBD), a cystine-rich domain (CRD), and two fibronectin III domains (FN III). The intracellular C-terminal domain encompasses a juxtamembrane region (JMS), a conserved tyrosine kinase (TK) domain, a sterile-a-motif domain (SAM), and a C-terminal zona occludens PSD95/DLG/ZO1 (PDZ) binding motif.

In 2008, it was initially noted that the *EPHA2* gene is associated with hereditary and age-related cataracts in Caucasians[9]. *EPHA2* is present in both human and murine crystalline structures, actively participating in guiding crystal cell movement and aligning fibers[10]. If *EPHA2* is disrupted through knockout methods, it noticeably changes the shape and arrangement of lens epithelial cells, leading to disturbances within the lens environment and ultimately causing cataract formation[11]. Remarkably, more than 20 variants of the *EPHA2* gene associated with various congenital cataract types have been documented over time. These variants are archived in the Cat-Map database (April 2022 version), primarily concentrated within the intracellular region. Curiously, the SAM surfaces as the most frequently altered domain in this context[12]. In this study, we identified a novel missense variant c.2780G>C of *EPHA2* (p.R957P) in a Chinese four-generation pedigree with autosomal dominant congenital cataract. The molecular basis underlying the pathogenicity of cataract caused by this variant was investigated.

SUBJECTS AND METHODS

Ethical Approval This study was approved by the Research Ethics Committee of the First Affiliated Hospital of Fujian Medical University (approval No.[2019]131). The procedures of the study conformed to the tenets of the Declaration of Helsinki and all subjects were informed of the research purpose before participating and signed the consent form.

Subjects and DNA Specimens A four-generation Chinese family affected with autosomal dominant CC was recruited at the First Affiliated Hospital of Fujian Medical University. Nineteen individuals took part in this study including 5 affected and 14 unaffected individuals. Clinical and ophthalmological examinations were performed on the affected individuals, as well as on the unaffected family members. Phenotype was documented by slit lamp photography. One hundred and twelve samples from ethnically matched control individuals were obtained prior to the study. Total genomic DNA was extracted from whole blood using the Wizard Genomic DNA purification kit (Promega, Beijing, China) according to the manufacturer's instructions.

Variant Screening and Haplotyping Analysis The variant screening strategy was based on the hot-spot variant regions of cataract-causing genes that cover about 80% of variants in inherited cataract, and the detail experimental process was the same as our previous study[13-14]. Briefly, the top 26 exons in 18 pathogenic genes were selected as the hot-spot mutation regions. These genes including *CRYAA*, *CRYAB*, *CRYBA1*, *CRYBA4*, *CRYBB1*, *CRYBB2*, *CRYBB3*, *CRYGC*, *CRYGD*, *CRYGS*, *GJA8*, *GJA3*, *HSF4*, *MIP*, *BFSP2*, *EPHA2*, *FYCO1*, and *PITX3*. The selected hot spot exons and splice junctions of these genes were amplified by polymerase chain reaction (PCR) from genomic DNA[13]. PCR products were purified and directly sequenced on an ABI 3730XL Automated Sequencer (PE Biosystems, Foster City, CA, USA) using the same PCR primers. When a suspected variant is found in the proband, it was confirmed among all of available other family members as well as in 112 normal unrelated individuals from the same ethnic background.

To further validate the co-segregation of the novel variant in *EPHA2*, the genotyping analysis was performed in available family members as the same as our previous study[13-14]. Briefly, three microsatellite markers (*D1S2736*, *D1S570*, and *D1S2672*) flanking *EPHA2* gene were selected. PCR products from each DNA sample were separated by gel electrophoresis with a fluoresence-based on ABI 3730 automated sequencer (Applied Biosystems) using ROX-500 as the internal lane size standard. The amplified DNA fragment lengths were assigned to allelic sizes with GeneMarker Version 2.4.0 software (SoftGenetics, State College, Pennsylvania, USA). Pedigree and haplotype data were managed using Cyrillic (version 2.1) software.

Bioinformatics Analysis Variant description followed the recommendation of the Human Genomic Variation Society (HGVS). The effects of novel missense variant on the encoded protein were further evaluated by Polymorphism Phenotyping v2 (PolyPhen-2)[15] and Sorting Intolerant From Tolerant v5.1.1 (SIFT)[16]. The pathogenicity of the variants was evaluated by

the standards and guidelines of American College of Medical Genetics and Genomics (ACMG)[17].

The 3-dimensional (3D) structure of wild type human EPHA2 was predicted with deep learning method by Robetta sever[18]. Swiss-Pdb Viewer software (Deep Viewer) 4.1.0 was used to analyze the structure. The mutant was induced in the modeled structure using the mutate tool and then selected the "best" rotamer on the new amino acid. Location in the structure, solvent accessibility of the residues, and change of surface electrostatic potential, gain/loss of H-bonds and steric clash were examined.

Cell Culture and Plasmids Transfection The full-length cDNA encoding EPHA2 (GenBank: NM_004431.5) with additional C-terminal Flag-tag (Flag-*EPHA2*-WT), and *EPHA2*-R957P mutant with C-termial HA-tag (HA-*EPHA2*-R957P) were synthesized and cloned into pcDNA3.1(+) (Invitrogen, Carlsbad, CA, USA) at *NheI* and *XhoI* sites. Both plasmids of wild type (pcDNA-Flag-*EPHA2*-WT) and mutant (pcDNA-HA-*EPHA2*-R957P) were confirmed through direct DNA sequencing.

COS-7 cells and human lens epithelial cells line (SRA 01/04) were cultured in Dulbecco's Modified Eagle's Medium (DMEM, Cat# C11885500BT, Gibco, USA) supplemented with 10% fetal bovine serum (FBS, Cat# ST30-3302, PAN, Germany), 100 U/mL penicillin, and 100 μg/mL streptomycin. The cultures were maintained at 37℃ in a humidified atmosphere of 95% air and 5% CO_2. Transient transfections of wild type and mutant plasmids were separately carried out using Polyethylenimine Linear MW40000 (PEI, rapid lysis; Cat# 40816ES02, YEASEN, China) according to the manufacturer's protocols.

Quantitative Real-time PCR Quantitative real-time PCR (qRT-PCR) was applied to detect the relative mRNA expression of wild-type and mutant of *EPHA2*. Briefly, total RNA was extracted by Trizol (Cat# R4801-01, Magen, China) from COS-7 cells after 48h transfection. RNA samples were reverse transcribed into cDNA using the All-in-one First-Strand Synthesis MasterMix (Cat# BM60502S, Baimeng Medicine, China). qRT-PCR was applied to detect the relative mRNA expression of wild-type and mutant of *EPHA2*. Briefly, total RNA was performed with a LightCycler 96 RealTime PCR Detection System (LightCycler 96, Roche, Switzerland) using Taq SYBR® Green qPCR Premix (Cat# BM60312S, Baimeng Medicine, China) with primers against *EPHA2* (Forward: 5'-TCAGAACAACTGAAGCCCCTG-3'; Reverse: 5'-CACAGGATGGATGGATCTCGG-3') and *GAPDH* (Forward: 5'-CACCCACTCCTCCACCTTTGA-3'; Reverse: 5'-TCTCTCTTCCTCTTGTGCTCTTGC-3'). Pre-denaturation at 95℃ for 30s and then reactions were run 40 cycles including denaturation at 95℃ for 10s, annealing at 60℃ for 30s and fluorescence signals collecting. Finally, the samples were entered the dissolution curve stage including 95℃ for 15s, 60℃ for 1min and 95℃ for 15s. All samples were normalized to median *GAPDH* expression. The qRT-PCR experiments were repeated three times.

Western Blot COS-7 cells or SRA 01/04 cells were grown on a 6-well plate, whole-cell extracts were obtained after 48h transfection and resolved by denaturing SDS-PAGE. In short, the collected cells were washed by the ice-cold phosphate buffer saline (PBS), and re-suspended in cell lysis buffer RIPA (Beyotime, P0013B) containing proteinase inhibitor PMSF (Beyotime, ST505, 1:100). After lysis on ice for 30min, the supernatant containing the target protein was collected by centrifugation (12 000 g) at 4℃. The protein concentration was quantified using the BCA assay with bovine serum albumin as standard protein. Total proteins were diluted in 4× loading buffer and denatured at 98℃ for 8min. Proteins 30 μg were separated by SDS-PAGE with 10% or 12% acrylamide and then transferred onto the a polyvinylidene fluoride (PVDF) membrane. PVDF membrane was next incubated with primary antibodies against HA (Affinity Biosciences, Cat# T0008), FLAG (Affinity Biosciences, Cat# T0053), EPHA2 (Cell Signaling Technology, Cat# 6997), β-catenin (Santa Cruz Biotechnology, Cat# sc-7963), E-cadherin (Santa Cruz Biotechnology, Cat# sc-8426) and β-Tubulin (Cell Signaling Technology, Cat# 2146S) at 4℃ overnight, diluting in a ratio of 1:1000, followed by horseradish peroxidase (HRP)-conjugated goat anti-rabbit (Affinity Biosciences, Cat# S0001, 1:5000) or mouse (Affinity Biosciences, OH, USA, Cat# S0002, 1:5000) secondary antibody at room temperature for 2h. The protein bands were visualized by enhanced chemiluminescence and the grey value was analyzed by Image J software. Each experiment was done at least three times independently.

Immunocytochemistry Assay COS-7 cells were cultured in confocal plates and fixed with 4% paraformaldehyde for 15min, followed by incubation for 1h in blocking buffer (5% normal goat serum, 0.3% Triton X-100 in PBS). Cells were then incubated with anti-HA (Affinity Biosciences, Cat# T0008), anti-Flag (Affinity Biosciences, Cat# T0053) primary antibody overnight at 4℃. After gently washing, the respective fluorescent secondary antibodies (Abcam, goat anti-mouse IgG H&L, Alexa Fluor 488, Cat# ab150113, 1:1000 or Abcam, goat anti-rabbit IgG H&L, Alexa Fluor 647, Cat# ab150079, 1:1000) were added and incubated with cells at 37℃ for 2h away from light. Hoechst 33342 (0.01 mg/mL) was used to stain the nuclei. Images were captured using a laser-scanning confocal microscope (Nussloch, Leica, Germany), merged and labeled by using Image J software.

Co-Immunoprecipitation Assay COS-7 cells were seeded into 10 cm dishes and transfected with plasmid encoding Flag-

tagged *EPHA2*-WT or HA-tagged *EPHA2*-R957P for 48h. Cells were harvested with co-immunoprecipitation assay (Co-IP) buffer (Beyotime, Cat# P0013). The lysates were then precleared with a 20 μL slurry of Protein A/G Beads (MCE, NJ, USA, Cat# HY-K0202) for 2h at 4℃. Precleared samples from wild-type and R957P group were incubated with flag or wild-type antibody overnight at 4℃, respectively. Then, 20 μL of protein A/G beads was added to the samples and incubated for 2h at 4℃. Samples were washed with co-IP buffer and boiled with 2× loading buffer for 10min at 98℃. The supernatants were carefully separated from the beads and loaded onto SDS-PAGE gels for Western blot analysis.

Wound Healing Assay The cell migration ability was analyzed by wound healing assay. SRA 01/04 cells with different transfections were cultured on 24-well plates at 37℃ and 5% CO_2 to reach confluence monolayers. A linear wound was created by using the fine end of sterile 100-μL pipette tips and washed three times with PBS to remove unattached cellular debris. The cells were then cultured in serum-free medium. Images of migrated cells were captured under inverted microscope at different times of cultivation (0, 12, and 24h). The gap distance of each monolayer was quantitatively evaluated using Image J. Cell migration rate was calculated as [0h scratch area-12h or 24h scratch area)/0h scratch area]×100%.

Zebrafish Maintenance and Breeding Zebrafish were bred in accordance with Fujian Medical University Animal Care and Use Committee protocols. The AB wild-type zebrafish were all maintained in E3 media (NaCl: 344 mg, KCl: 15.2 mg, $CaCl_2{\cdot}2H_2O$: 58 mg, $MgSO_4{\cdot}7H_2O$: 98 mg) in the same tank. The male to female ratio was 2:1, light:dark (L:D) cycle was in a 14:10. The embryos were collected and raised at 28.3℃ and staged in hours post fertilization (hpf) or days post fertilization (dpf). PTU 0.003% (300 mg of phenylthiourea and fix the volume to 1 L of E3 media) was added to inhibit melanogenesis.

Injections of mRNA into Zebrafish Embryos The 5'-capped mRNA of wild-type and mutant of *EPHA2* were synthesized from pcDNA-Flag-*EPHA2*-WT and pcDNA-HA-*EPHA2*-R957P using mMESSAGE mMACHINE T7 kit (Ambion), respectively. Zebrafish embryos were divided into four groups: Control (no injection), enhanced green fluorescent protein (EGFP mRNA), *EPHA2*-WT (EGFP and h*EPHA2*-WT mRNA) and *EPHA2*-R957P (EGFP and h*EPHA2*-R957P mRNA). A total of 100-500 pg of mRNA purified with the RNeasy mini kit (Qiagen, Austin, TX, USA) were injected into the one-cell stage embryos. Living embryos were observed under a stereo microscope (Nikon, SMZ800N, Japan) and photos were taken. Three separate eye phenotypic categories including vacuoles at 28 hpf, microphthalmia at 48 hpf, lens opacity at 3 dpf, and 4 dpf were recorded.

Statistical Analysis All the experiments indicated above were implemented at least 3 times. The data are presented as mean±standard deviation (SD). The statistical analysis was performed by R4.1.2 and by GraphPad Prism 7.0 (San Diego, CA, USA). The differences between two groups were analyzed by Welch's *t*-test, whereas that among three or more groups by one-way analysis of variance (ANOVA). The differences in counting data between groups were compared using Fisher's exact test. $P<0.05$ was considered statistically significant.

RESULTS

Clinical Features of a Chinese Cataract Family and Bioinformatics Analysis There are five affected individuals with congenital cataract in the Chinese four-generation family. This pedigree demonstrates the autosomal dominant inheritance pattern based on clinical histories (Figure 1A). The proband (IV: 2) was a 4-year-old boy who suffered posterior polar opacity in bilateral lens (Figure 1B). His visual acuity was 0.3 in both eyes and his best corrected visual acuity ranged from 0.5 to 0.7. The other four affected members showed similar cataracts and underwent cataract surgeries soon after the diagnosis. There were no other ocular or systemic abnormalities in these cases.

By sequencing the hot-spot variant regions of cataract-causing candidate genes, a heterozygous c.2870G>C variation in exon 17 of *EPHA2* was detected in the proband of this family (Figure 1C), which changed arginine to proline at codon 957 (p.R957P) in the SAM domain of EPHA2 protein (Figure 1D). Since this variant has not been reported previously, we deposited it in the online human variation database LOVD3: https://databases.lovd.nl/shared/variants/0000167021#00007156. The multiple sequence alignments showed that this amino acid is highly conserved across various species (Figure 1E). This variant co-segregated with the phenotype in all affected family members and was not observed in unaffected family members or in the unrelated healthy population. Haplotype analysis showed that the affected individuals in the family shared a common haplotype with markers *D1S2736*, *D1S570*, and *D1S2672* flanking *EPHA2* locus (Figure 1A). The h*EPHA2*/p.R957P variant has not been previously reported and was also absent in the public databases including dbSNP, 1000 Genomes, ExAC and gnomAD. It was predicted with high confidence to be "possibly damaging" and "deleterious" by both Polyphen-2 (score=0.958) and SIFT (score=0), respectively. The clinical significances of this variant was classified as "pathogenic" with the criterions of PS3, PM1, PM2, PP1 and PP3 by Inter Var software based on the criteria recommended by ACMG/AMP guide-lines[13]. In addition, the molecular surface structure of EPHA2 may be changed by R957P variant through the prediction of Robetta sever and Swiss-Pdb Viewer (Figure 1F)[18].

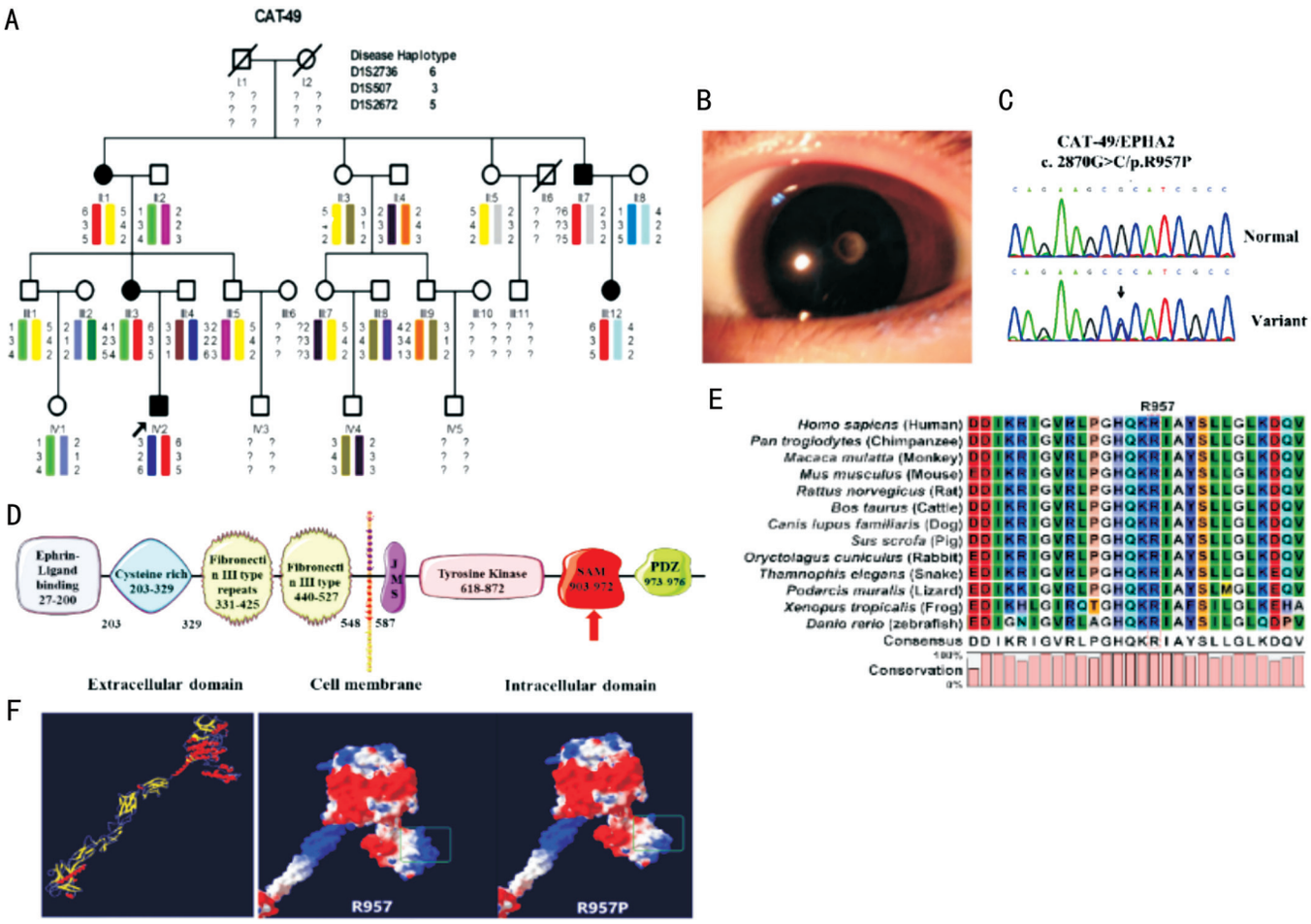

Figure 1 *EPHA2* variant (p.R957P) in Family CAT-49 with autosomal dominant congenital posterior polar cataract A: Pedigree of CAT-49 family. Haplotype segregating with the disease is red boxed with markers *D1S2736*, *D1S507*, and *D1S2672*. Squares and circles symbolize males and females, respectively. Filled symbols denote affected status. The proband is labeled by a black arrow. B: Slit lamp photograph of the left eye of the patient (IV: 2) with posterior polar opacity in lens. C: DNA sequence of affected and unaffected individuals. A novel heterozygous variant (c.2870G>C, p.R957P) was detected in exon 17 of *EPHA2* in affected individuals. The variant was not detected in the unaffected members in the family or the 112 unrelated normal controls. D: Schematic diagram of EPHA2 structure. The amino acid residue R975 was located in SAM domain (orange arrow) of EPHA2. E: Multiple sequences alignment of EPHA2 is shown from various species, including human (NP_004422.2), chimpanzee (XP_016810290.1), Rhesus monkey (NP_001035768.1), mouse (NP_034269.2), rat (NP_001102447.1), cattle (NP_001192660.1), dog (XP_038516156.1), pig (XP_005665094.1), rabbit (XP_002722370.1), snake (XP_032088153.1), lizard (XP_028597216.1), frog (NP_001006765.1) and zebrafish (NP_571490.1). F: Structure homology modeling and comparison of *EPHA2* wild-type and p.R957P mutant. The structure model of human EPHA2 protein was predicted by Robetta sever (left), and alteration of surface electrostatic potential in mutant (right) comparing to that of wild-type (middle). The molecular surface is colored according to electrostatic potential using the Swiss-PdbViewer, with red-white-blue corresponding to acidic-neutral-basic potential, and the blue dotted circle represents the region of significant alteration of surface electrostatic potential.

Effect of R957P Variant on *EPHA2* Expression To investigate whether the c.2870G>C (p.R957P) variant affects *EPHA2* expression, COS-7 cells were transiently transfected with Flag-tagged *EPHA2*-WT or HA-tagged *EPHA2*-R957P plasmid, respectively (Figure 2A). In Western blotting experiments, anti-Flag antibody, anti-HA antibody and anti-EPHA2 antibody were used to detect protein bands with a molecular weight similar to EPHA2 protein (130 kDa; Figure 2B-2C). The quantitative analysis results showed that compared with the Empty group, the WT group overexpressing wild-type *EPHA2* showed an increase in EPHA2 protein levels. However, compared with the WT group, the R957P group overexpressing variant *EPHA2* showed a statistically significant decrease in EPHA2 protein levels (Figure 2D, $P<0.001$), suggesting that p.R957P variant only affected EPHA2 protein expression post-transcriptionally.

***EPHA2*/p.R957P Variant Affected the Subcellular Localization and Protein-Protein Interaction of EPHA2** As illustrated in Figure 3A, Flag-tagged wild-type EPHA2 manifested as membrane localization, while HA-tagged variant

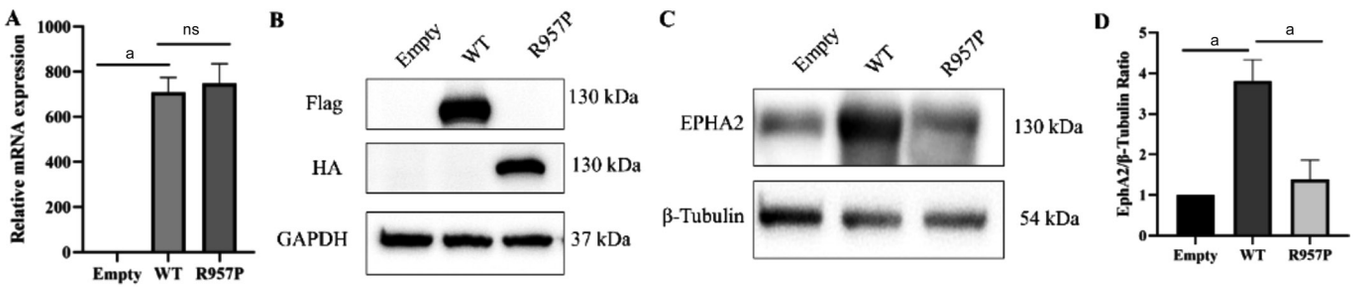

Figure 2 Expression analysis of *EPHA2*-WT and *EPHA2*-R957P in COS-7 cells A: mRNA expression of *EPHA2* analyzed by qRT-PCR. There was no statistical difference in the expression level of *EPHA2* mRNA between WT and R957P group, with *GAPDH* as loading control. n=3, ^{a}P<0.001, ns: P>0.05. B-C: Anti-Flag antibody, anti-HA antibody, and anti-EPHA2 antibody were used to detect protein bands with a molecular weight similar to EPHA2 protein (130 kDa) by Western blot. D: The expression of EPHA2 protein in R957P group was lower than that in WT group, taking β-Tubulin as loading control. n=3, ^{a}P<0.001. EPHA2: Ephrin type-A receptor 2; WT: Wild type.

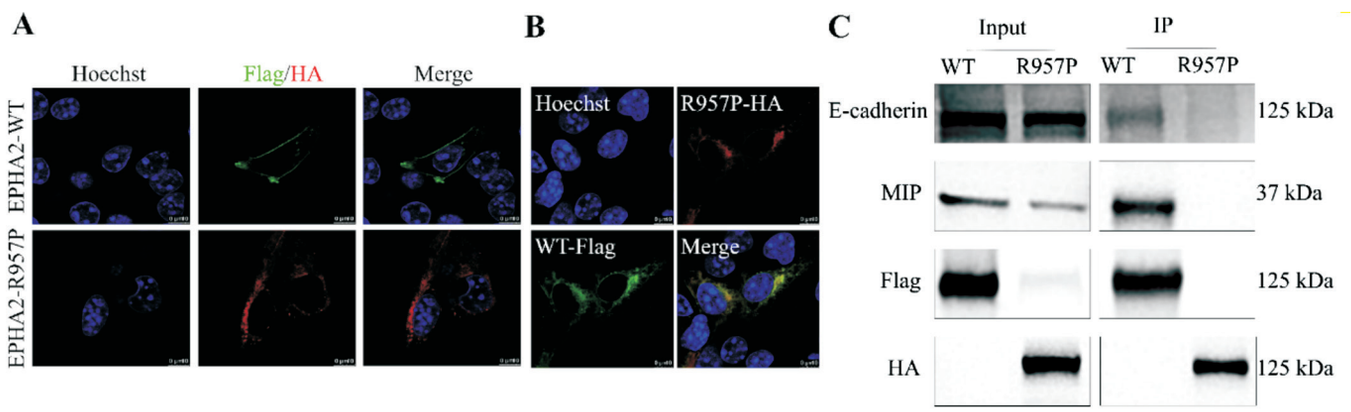

Figure 3 The effect of R957P variant on the subcellular localization and protein-protein interaction of EPHA2 A: Subcellular localization of wild type and mutant EPHA2 protein. The confocal microscope showed that the EPHA2-WT mainly existed on the cell membrane in COS-7 cells (green), while the EPHA2-R957P presented a diffuse perinuclear distribution pattern (red). B: Partial co-localization of p.R957P mutant and wild-type EPHA2 (yellow puncta). Scale bar: 10 μm. C: *EPHA2*/p.R957P destroyed the interaction between EPHA2 and other membrane proteins. Co-IP assay indicated the interaction existed between EPHA2-WT and membrane proteins (E-cadherin and MIP) in COS-7 cells, which was absent in R957P group. EPHA2: Ephrin type-A receptor 2; WT: Wild type; Co-IP: Co-immunoprecipitation assay.

EPHA2 represented cytoplasmic localization that distributed around the nucleus. However, in COS-7 cells co-transfected with Flag-*EPHA2*-WT and HA-*EPHA2*-R957P group, both fluorescence-labeled Flag and HA puncta scattered around the nucleus in cytoplasm, and the co-localization of these two puncta was observed, indicating that p.R957P mutant altered the membrane distribution pattern of wild-type EPHA2 (Figure 3B).

The effects of p.R957P variant on the interaction between EPHA2 and membrane proteins including E-cadherin[19] and MIP[20] were further explored. We observed positive interactions between the wild-type EPHA2 with E-cadherin and MIP (Figure 3C). However, the interactions between the mutant EPHA2 and E-cadherin or MIP were not detectable, suggesting that p.R957P variant destroyed their interaction. Together with the results from subcellular localization analysis, the dissociation between EPHA2 and lens proteins may be due to its transportation to cytoplasm induced by p.R957P variant.

***EPHA2*/p.R957P Variant Promoted Cell Migration in SRA 01/04 Cells** Subsequently, SRA 01/04 expressing wild type or p.R957P variant *EPHA2* were constructed to determine the effects of *EPHA2* variant on the biological activities of lens epithelial cells. Compared with empty plasmid control, cells transfected with *EPHA2*-WT showed no significant difference in migration after 12 and 24h. However, cells expressing *EPHA2*/p.R957P mutant migrated more than 2-fold faster than those expressing *EPHA2*-WT at 12 or 24h after transfection (Figure 4A-4B). Furthermore, the protein levels of β-catenin and E-cadherin were significantly down-regulated in SRA 01/04 cells with transfection of *EPHA2*-R957P plasmid compared with that in WT group (Figure 4C-4D), indicating that epithelial-to-mesenchymal (EMT) was activated, which might explain the inhibitory effect on cell migration induced by p.R957P variant.

***hEPHA2* R957P Mutant Resulted in Lens Opacity in Zebrafish** As illustrated in Table 1 and Figure 5, when ectopically expressing R957P mutant, 8.3% (10/121) zebrafish

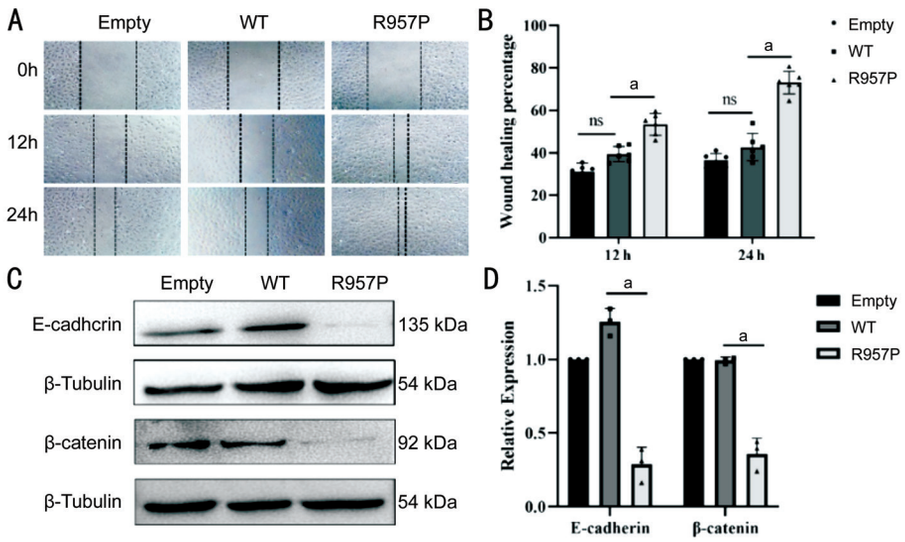

Figure 4 R957P variant promoted cell migration A-B: Wound healing assay detected cell mobility. The percentage of wound healing area in R957P group increased significantly comparing with that in WT group 12 or 24h after scratch. *n*=6, ^{a}P<0.001, ns: *P*>0.05. C-D: Western blot analysis of EMT-related proteins. The quantitative analysis showed that EPHA2/p.R957P variant significantly down-regulated the expression levels of E-cadherin and β-catenin. *n*=3, ns: *P*>0.05, ^{a}P<0.001. EPHA2: Ephrin type-A receptor 2; WT: Wild type; EMT: Epithelial-to-mesenchymal.

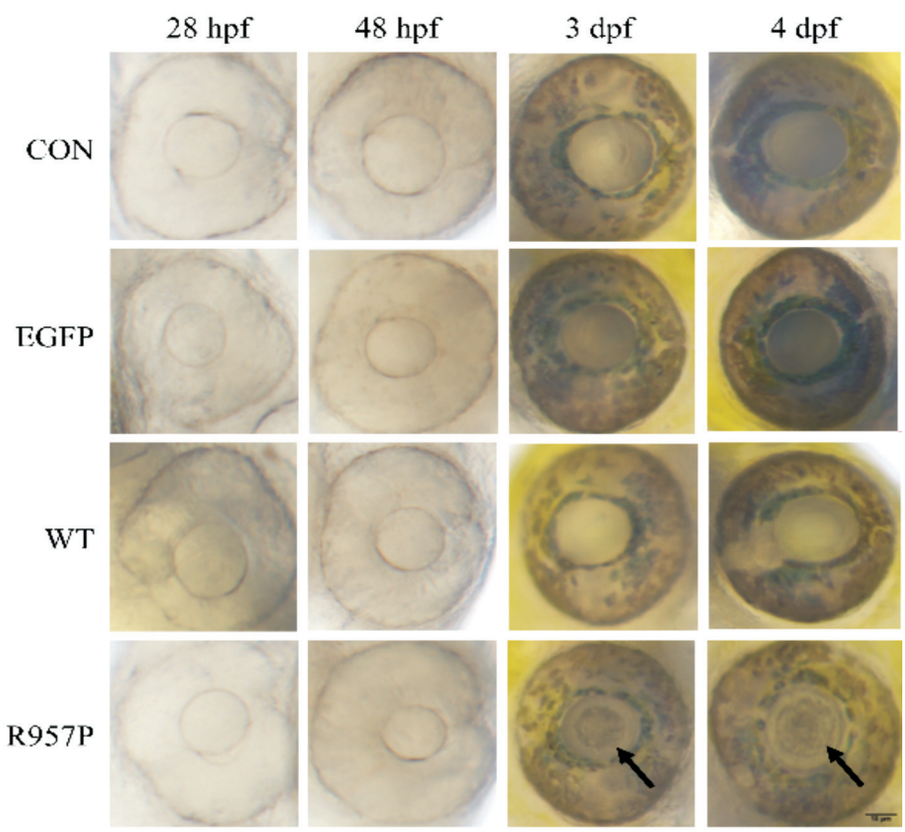

Figure 5 *EPHA2*/p.R957P mutant leaded to cataracts in zebrafish Zebrafish injected with *hEPHA2* R957P mRNA into single-cell embryos showed central lens opacity in 3 and 4 dpf. Scale bar: 10 μm. CON: Control; EGFP: Enhanced green fluorescent protein; WT: Wild type; hpf: Hours post fertilization; dpf: Days post fertilization.

embryos exhibited obvious cataract phenotype including a central cloudy region at 3 dpf, while 35.5% (43/121) embryos displayed the opacity ranging from a central area to larger region encompassing most of the lens at 4 dpf. In contrast, almost all of lens from wild-type embryos and embryos with ectopic EGFP expression were completely transparent at 3 and 4 dpf. Interestingly, 1.25% (1/80) embryos ectopically expressing human wild-type *EPHA2* displayed the lens opacity at 3 and 4 dpf. No lens opacity was observed in the control group or embryos injected with EGFP, WT, and mutant *EPHA2* groups at 28 and 48 hpf. These results suggested that the incidence of cataract phenotype in h*EPHA2* p.R957P

Table 1 Prevalence of different eye phenotypes in zebrafish at the different development stages

Phenotypes	28 hpf	48 hpf	3 dpf	4 dpf
Control	0/100	0/100	0/100	0/100
EGFP	0/100	0/100	0/100	0/100
Wild type	0/80	0/80	1/80 (1.25%)	1/80 (1.25%)
R957P	0/121	0/121	10/121 (8.3%)	43/121 (35.5%)
P	-	-	0.053	<0.0001

EGFP: Enhanced green fluorescent protein; hpf: Hours post fertilization; dpf: Days post fertilization.

mutant group is significantly higher than that of WT group (Fisher exact test, $P<0.001$), supporting the causative effect of p.R957P on the development of cataract.

DISCUSSION

Variants in the *EPHA2* gene can cause congenital and age-related cataracts[4,21-22]. Herein, based on screening the variant hot-spot regions of cataract-causing genes, a novel missense variant *EPHA2* c.2870G>C was identified in a four-generation Chinese family with the posterior polar cataracts. This pathogenic variant was further confirmed by haplotype and co-segregation analysis. The c.2870G>C transversion leads to the substitution of a nonpolar and hydrophobic proline residue for a positive charge and highly conserved arginine residue at codon 957 (p.R957P) which located at the SAM domain of EPHA2. Since human *EPHA2* was first identified as the causative gene responsible for cataracts that map to 1p36 in 2008[9], twenty-five variants were reported in different populations so far (https://cat-map.wustl.edu/; Table 2)[1,4,9,21,23-40]. These variants are located in different domains of EPHA2, including CRD, FN III, JMS, TK, SAM and PDZ domains. Among of them, the SAM domain is the most frequently variant region (41.67%, 10/24), which suggests that the SAM domain of EPHA2 may be important in EPHA2 function. In fact, this domain exists in all Eph receptors and is known as an interaction motif, which form homotypic and heterotypic dimers or oligomers to mediate protein-protein interactions[41]. Variants within SAM domain, such as R957D, result in attenuated binding affinity compared to the wild-type proteins[42]. The research on p.R957H as a somatic variant in age-related cataract[12] and R957C associated with ovarian cancer[8] both reveals that mutations in SAM will alter the protein's function.

To gain insights into the potential mechanism of how *EPHA2*/p.R957P mutant causes cataract, we have investigated its functional defects which may be involved in both gain and loss of function of EPHA2. The effect of R957P variant on EPHA2 expression was first analyzed. The results showed that the expression of *EPHA2*/p.R957P mutant significantly decreased at protein level through post-translational modifications as well as that of the other SAM domain variants of EPHA2[43]. The c.G668D variant in the kinase domain of EPHA2 also led to a relatively low mutant protein level, which was considered as a EPHA2 loss-of function[21]. In addition to variants in the coding region of EPHA2, non-coding SNP rs6603883 located in the PAX2-binding motif within the promoter region of EPHA2 declined the EPHA2 protein levels through the translational regulation. This down-regulation of EPHA2 levels alters the downstream MAPK/AKT pathway and affects other extracellular matrix (ECM) and cytoskeletal genes to cause cataracts[44].

The EPHA2 protein localizes to the cell membrane in both lens fiber cells and lens epithelial cells *in vivo*[45-46]. However, some variants of *EPHA2* were reported to alter subcellular distribution[21]. Indeed we also observed that the *EPHA2*/p.R957P mutant mis-localized to the perinuclear space of cells. What's more, this mutant may also influence membrane localization and subcellular distribution of the wild-type EPHA2 when co-expressed in COS-7 cells. Major intrinsic protein or aquaporin-0 (MIP/AQP0), one of the causative genes of congenital cataracts, functions as a water channel and an adhesion molecule in mediating the formation of thin junctions between lens fibers[47]. We observed that the p.R957P variant destroyed the interaction between EPHA2 and MIP by Co-IP assay, implying that this mutant could alter the MIP/AQP0 localization. Cheng *et al*[48] reported that the localization of MIP/AQP0 is disrupted in *EPHA2*$^{-/-}$ cortical lens fibers. Thus, these data suggest that *EPHA2*/p.R957P mutant could lead to cellular disorganization and eventual lens opacity.

The coordinated elongation and migration of cohorts of lens fiber cells plays an key role in the development of lens sutures[49]. *EPHA2*-null lenses have displayed the sutural defects and disturbances in the surface patterning of individual fiber cells, implying that EPHA2 has a role in the directed migration of lens fiber cells[50]. Murugan and Cheng[51] reported that the wild-type *EPHA2* promoted the migration of mouse lens epithelial αTN4-1 cells in the absence of ligand stimulation, and that the variants in SAM domain diminished this activity. Our results of wound healing assay revealed that the overexpression of wild-type *EPHA2* in SRA 01/04 cells had no effect on cell migration. However, unlike the inhibition of cell migration caused by the other SAM domain variants (T940I, G948W, V972GfsX39 and splicing mutant c.2826-9G>A) of *EPHA2*[25], the R957P mutant exhibit significantly enhanced cell migration compared with wild-type in SRA 01/04 cells, suggesting that the disease-causing R957P variant in humans likely acts by gain-of-function. Furthermore, *EPHA2*/p.R957P mutant reduced notably the expressions of both E-cadherin and β-catenin. E-cadherin may recruit β-catenin to form complexes that are involved in EMT[52]. They are also required for cell adhesion during lens development and have shown to play an important part in the coordination

Table 2 Variants in *EPHA2* known to cause congenital cataract

No.	Exon/ intron	DNA change	Protein change	Mutational pattern	Mutated domain	Inheritance	Phenotype	Origin	Year	Reference
1	Ex3	c.649G>C	p.G217R	Missense	CRD	AD	Nuclear and microphthalmos and microcornea	Spain	2021	[23]
2	Ex3	c.785G>A	p.C262Y	Missense	CRD	AR	Lamellar, microcornea and nystagmus	India	2020	[1]
3	Ex4	c.855A>G	p.K282E	Missense	Non protein region	AD	Nuclear, cortical	UK	2016	[24]
4	Ex5	c.988dupT	p.S330FfsX51	Frameshift	FN III	Sporadic	NA	Sri Lanka	2018	[25]
5	Ex5	c.1046C>T	p.T349M	Missense	FN III	AD	Nuclear	China	2014	[26]
6	Ex5	c.1059_1060dupCA	p.S354MfsX40	Frameshift	FN III	N/A	Nuclear, cortical and microcornea	UK	2014	[27]
7	Ex6	c.1315C>T	p.P439S	Missense	FN III	AR	Pediatric	Saudi Arabia, USA	2017	[28]
8	Ex6	c.1405T>C	P.Y469H	Missense	FN III	AR	Posterior polar	Saudi Arabia, USA	2012/2015	[29-30]
9	Ex7	c.1532C >T	p.T511M	Missense	FN III	AD	Total	China	2019	[31]
10	Ex10	c.1751C>T	p.P584L	Missense	JMS	AD	Irregular nuclear and cortical	Australia, UK	2013/2021	[32-33]
11	Ex11	c.2003G>A	p.G668D	Missense	TK	AD	Posterior subcapsular	China	2019	[21]
12	Ex11	c.2007G>T	p.Q669H	Missense	TK	AD	Pediatric	Saudi Arabia, USA	2017	[28]
13	Ex14	c.2353G>A	p.A785T	Missense	TK	AR	Nuclear	Pakistan	2010/2021	[4, 34]
14	Ex15	c.2668C>T	p.R890C	Missense	SAM	AD	Posterior polar	China	2013	[35]
15	Ex16	c.2710delG	p.V904CfsX36	Frameshift	SAM	AR	Nuclear	Pakistan	2021	[4]
16	Ex16	c.2800G>A	p.E934K	Missense	SAM	Sporadic	Cortical	China	2016	[36]
17	Ex16	c.2803A>T	p.K935X	Missense	SAM	Sporadic	Total	China	2016	[36]
18	Ex16	c.2819C>T	p.T940I	Missense	SAM	AD	Posterior polar	China	2009	[37]
19	IVS16	c.2825+1G>A	p.D942EfsX1	Splice site	SAM	AD	Pediatric	China	2016	[38]
20	IVS16	c.2826-9G>A	p.D942EfsX71	Splice site	SAM	AD	Nuclear, cortical, total and microphthalmia	China, Mexico, Australia, UK	2009/2013/ 2018/2021	[22,33,37,39]
21	Ex17	c.2842G>T	p.G948W	Missense	SAM	AD	Posterior subcapsular	USA	2008	[9]
22	Ex17	c.2870G>C	P.R957P	Missense	SAM	AD	Posterior subcapsular	China	2024	This study
23	Ex17	c.2875G>A	p.A959T	Missense	SAM	AD	Posterior subcapsular	Australia	2013	[33]
24	Ex17	c.2915_2916delTG	p.V972GfsX39	Frameshift	SAM	AD	Posterior polar	China	2009	[37]
25	Ex17	c.2925dupC	p.I976HfsX37	Frameshift	PDZ	AD	Cataract and glaucoma	USA	2014	[40]

AD: Autosomal dominant; AR: Autosomal recessive; Ex: Exon; IVS: Intervening sequence; CRD: A cystine-rich domain; FN III: Fibronectin III domains; JMS: Juxtamembrane region; TK: Tyrosine kinase; SAM: Sterile-a-motif domain; PDZ: PSD95/DLG/ZO1.

of morphogenesis[53-54]. These data suggest that *EPHA2*/p.R957P mutant could lead to human lens epithelial cell trans differentiation and subsequent cataract formation.

To functionally validate pathogenicity, we also performed the ectopic expression of human wild-type or R957P mutant *EPHA2* in zebrafish. The incidence of cataract phenotype in *hEPHA2* p.R957P mutant group increased from 8.3% (10/121) at 3 dpf to 35.5% (43/121) at 4 pdf with statistical significance, which further confirmed that this mutant may contribute to the development of cataracts. Morpholino knockdown of *EPHA2a*/*EPHA2b* in zebrafish resulted in significantly reduced eye size and cataract formation[23]. However, we observed no smaller eyes and lens in embryos injected with WT h*EPHA2* and R957P h*EPHA2* than that in the normal control zebrafish. Several groups have reported that disruption of the mouse *EPHA2* gene has been exerted dramatically variable effects on lens phenotype ranging from severe progressive cataract formation to subtle nuclear opacities or clear lenses with smaller equatorial diameter and disturbed lens refractive properties[51].

In summary, our study reported a novel *EPHA2* gene variant (c.2870G>C, p.R957P) in the SAM domain that results in a congenital posterior polar cataract in a four-generation Chinese family. Functional defects of this variant studies revealed that p.R957P variant generated variant or unstable EPHA2 protein, changed subcellular localization of the EPHA2 from the cell membrane to the cytoplasm, destroyed the interaction between EPHA2 and membrane proteins and promoted cell migration. β-catenin and E-cadherin expression were down-regulated that further triggered EMT. The dysregulated function above may be primary causes involved in the formation of cataracts.

ACKNOWLEDGEMENTS

Authors' contributions: Yang JH, Zhang JJ, and Cao ZF conceived and designed the experiments. Zhang JJ, Cao ZF, and Zhou BT performed the experiments and prepared the figures and tables. Ye Q, Li Z, Lin S, Chen XL, and Zhang NW collected the data from the samples. Zhang JJ and Zhou BT contributed to writing the manuscript. Zhu YH, Ma X, Ye Q, and Yang JH reviewed the manuscript. All authors contributed to discussed the manuscript at various stages.

Foundations: Supported by the Natural Science Foundation of Fujian Province (No.2021J01229); National Key Research and Development Program of China (No.2016YFC1000307).

Conflicts of Interest: Zhang JJ, None; **Cao ZF,** None; **Zhou BT,** None; **Yang JH,** None; **Li Z,** None; **Lin S,** None; **Chen XL,** None; **Zhang NW,** None; **Ye Q,** None; **Ma X,** None; **Zhu YH,** None.

REFERENCES

1 Kandaswamy DK, Prakash MVS, Graw J, Koller S, Magyar I, Tiwari A, Berger W, Santhiya ST. Application of WES towards molecular investigation of congenital cataracts: identification of novel alleles and genes in a hospital-based cohort of South India. *Int J Mol Sci* 2020;21(24):9569.

2 Beheshtnejad A, Hashemian H, Kakaie S, Mahdavi A, Naderan M. Outcomes of the infantile cataract surgery: case series with a 5-year follow-up. *Int Ophthalmol* 2022;42(2):541-547.

3 GBD Blindness and Vision Impairment Collaborators, Vision Loss Expert Group of the Global Burden of Disease Study. Causes of blindness and vision impairment in 2020 and trends over 30 years, and prevalence of avoidable blindness in relation to VISION 2020: the Right to Sight: an analysis for the Global Burden of Disease Study. *Lancet Glob Health* 2021;9(2):e144-e160.

4 Jarwar P, Sheikh SA, Waryah YM, Ujjan IU, Riazuddin S, Waryah AM, Ahmed ZM. Biallelic variants in *EPHA2* identified in three large inbred families with early-onset cataract. *Int J Mol Sci* 2021;22(19):10655.

5 Jarwar P, Waryah YM, Rafiq M, Waryah AM. Association of single nucleotide polymorphism variations in *CRYAA* and *CRYAB* genes with congenital cataract in Pakistani population. *Saudi J Biol Sci* 2022;29(4):2727-2732.

6 Deng M, Tong R, Zhang Z, Wang T, Liang C, Zhou X, Hou G. EFNA3 as a predictor of clinical prognosis and immune checkpoint therapy efficacy in patients with lung adenocarcinoma. *Cancer Cell Int* 2021;21(1):535.

7 Lindberg RA, Hunter T. cDNA cloning and characterization of Eck, an epithelial cell receptor protein-tyrosine kinase in the eph/elk family of protein kinases. *Mol Cell Biol* 1990;10(12):6316-6324.

8 Wang Y, Shang Y, Li J, Chen W, Li G, Wan J, Liu W, Zhang M. Specific Eph receptor-cytoplasmic effector signaling mediated by SAM-SAM domain interactions. *Elife* 2018;7:e35677.

9 Shiels A, Bennett TM, Knopf HL, Maraini G, Li A, Jiao X, Hejtmancik JF. The EPHA2 gene is associated with cataracts linked to chromosome 1p. *Mol Vis* 2008;14:2042-2055.

10 Cheng C, Ansari MM, Cooper JA, Gong X. EphA2 and Src regulate equatorial cell morphogenesis during lens development. *Development* 2013;140(20):4237-4245.

11 Cheng C, Gong X. Diverse roles of Eph/ephrin signaling in the mouse lens. *PLoS One* 2011;6(11):e28147.

12 Bennett TM, M'Hamdi O, Hejtmancik JF, Shiels A. Germ-line and somatic EPHA2 coding variants in lens aging and cataract. *PLoS One* 2017;12(12):e0189881.

13 Cao Z, Zhu Y, Liu L, Wu S, Liu B, Zhuang J, Tong Y, Chen X, Xie Y, Nie K, Lu C, Ma X, Yang J. Novel mutations in HSF4 cause congenital cataracts in Chinese families. *BMC Med Genet* 2018;19(1):150.

14 Zhuang J, Cao Z, Zhu Y, Liu L, Tong Y, Chen X, Wang Y, Lu C, Ma X, Yang J. Mutation screening of crystallin genes in Chinese families with congenital cataracts. *Mol Vis* 2019;25:427-437.

15 Adzhubei IA, Schmidt S, Peshkin L, Ramensky VE, Gerasimova A, Bork P, Kondrashov AS, Sunyaev SR. A method and server for predicting damaging missense mutations. *Nat Methods* 2010;7(4):248-249.

16 Zheng C, Wang Y, Luo Y, Pang Z, Zhou Y, Min L, Tu C. Synchronous lung and multiple soft tissue metastases developed from osteosarcoma of tibia: a rare case report and genetic profile analysis. *BMC Musculoskelet Disord* 2022;23(1):74.

17 Dericquebourg A, Fretigny M, Chatron N, Tardy B, Zawadzki C, Chambost H, Vinciguerra C, Jourdy Y. Whole F9 gene sequencing identified deep intronic variations in genetically unresolved hemophilia B patients. *J Thromb Haemost* 2023;21(4):828-837.

18 Baek M, DiMaio F, Anishchenko I, *et al*. Accurate prediction of protein structures and interactions using a three-track neural network. *Science* 2021;373(6557):871-876.

19 Kurose H, Ueda K, Kondo R, Ogasawara S, Kusano H, Sanada S, Naito Y, Nakiri M, Nishihara K, Kakuma T, Akiba J, Igawa T, Yano H. Elevated expression of EPHA2 is associated with poor prognosis after radical prostatectomy in prostate cancer. *Anticancer Res* 2019;39(11):6249-6257.

20 Sun W, Xu J, Gu Y, Du C. The relationship between major intrinsic protein genes and cataract. *Int Ophthalmol* 2021;41(1):375-387.

21 Zhai Y, Zhu S, Li JY, Yao K. A novel human congenital cataract mutation in EPHA2 kinase domain (p.G668D) alters receptor stability and function. *Invest Ophthalmol Vis Sci* 2019;60(14):4717-4726.

22 Dave A, Craig JE, Alamein M, Skrzypiec K, Beltz J, Pfaff A, Burdon KP, Ercal N, de Iongh RU, Sharma S. Genotype, age, genetic background, and sex influence Epha2-related cataract development in mice. *Invest Ophthalmol Vis Sci* 2021;62(12):3.

23 Fernández-Alcalde C, Nieves-Moreno M, Noval S, Peralta JM, Montaño VEF, del Pozo Á, Santos-Simarro F, Vallespín E. Molecular and genetic mechanism of non-syndromic congenital cataracts. mutation screening in Spanish families. *Genes* 2021;12(4):580.

24 Musleh M, Hall G, Lloyd IC, Gillespie RL, Waller S, Douzgou S, Clayton-Smith J, Kehdi E, Black GC, Ashworth J. Diagnosing the cause of bilateral paediatric cataracts: comparison of standard testing with a next-generation sequencing approach. *Eye (Lond)* 2016;30(9):1175-1181.

25 Javadiyan S, Lucas SEM, Wangmo, Ngy M, Edussuriya K, Craig JE, Rudkin A, Casson R, Selva D, Sharma S, Lower KM, Meucke J, Burdon KP. Identification of novel mutations causing pediatric cataract in Bhutan, Cambodia, and Sri Lanka. *Mol Genet Genomic Med* 2018;6(4):555-564.

26 Sun W, Xiao X, Li S, Guo X, Zhang Q. Exome sequencing of 18 Chinese families with congenital cataracts: a new sight of the NHS

gene. *PLoS One* 2014;9(6):e100455.

27 Gillespie RL, O'Sullivan J, Ashworth J, Bhaskar S, Williams S, Biswas S, Kehdi E, Ramsden SC, Clayton-Smith J, Black GC, Lloyd IC. Personalized diagnosis and management of congenital cataract by next-generation sequencing. *Ophthalmology* 2014;121(11):2124-2137.e1-2.

28 Patel N, Anand D, Monies D, *et al*. Novel phenotypes and loci identified through clinical genomics approaches to pediatric cataract. *Hum Genet* 2017;136(2):205-225.

29 Aldahmesh MA, Khan AO, Mohamed JY, Hijazi H, Al-Owain M, Alswaid A, Alkuraya FS. Genomic analysis of pediatric cataract in Saudi Arabia reveals novel candidate disease genes. *Genet Med* 2012;14(12):955-962.

30 Khan AO, Aldahmesh MA, Alkuraya FS. Phenotypes of recessive pediatric cataract in a cohort of children with identified homozygous gene mutations (an American ophthalmological society thesis). *Trans Am Ophthalmol Soc* 2015;113:T7.

31 Li S, Zhang J, Cao Y, You Y, Zhao X. Novel mutations identified in Chinese families with autosomal dominant congenital cataracts by targeted next-generation sequencing. *BMC Med Genet* 2019;20(1):196.

32 Harding P, Toms M, Schiff E, Owen N, Bell S, Lloyd IC, Moosajee M. *EPHA2* segregates with microphthalmia and congenital cataracts in two unrelated families. *Int J Mol Sci* 2021;22(4):2190.

33 Dave A, Laurie K, Staffieri SE, Taranath D, MacKey DA, Mitchell P, Wang JJ, Craig JE, Burdon KP, Sharma S. Mutations in the EPHA2 gene are a major contributor to inherited cataracts in South-Eastern Australia. *PLoS One* 2013;8(8):e72518.

34 Kaul H, Riazuddin SA, Shahid M, Kousar S, Butt NH, Zafar AU, Khan SN, Husnain T, Akram J, Hejtmancik JF, Riazuddin S. Autosomal recessive congenital cataract linked to EPHA2 in a consanguineous Pakistani family. *Mol Vis* 2010;16:511-517.

35 Shentu XC, Zhao SJ, Zhang L, Miao Q. A novel p.R890C mutation in EPHA2 gene associated with progressive childhood posterior cataract in a Chinese family. *Int J Ophthalmol* 2013;6(1):34-38.

36 Li D, Wang S, Ye H, Tang Y, Qiu X, Fan Q, Rong X, Liu X, Chen Y, Yang J, Lu Y. Distribution of gene mutations in sporadic congenital cataract in a Han Chinese population. *Mol Vis* 2016;22:589-598.

37 Zhang T, Hua R, Xiao W, Burdon KP, Bhattacharya SS, Craig JE, Shang D, Zhao X, MacKey DA, Moore AT, Luo Y, Zhang J, Zhang X. Mutations of the EPHA2 receptor tyrosine kinase gene cause autosomal dominant congenital cataract. *Hum Mutat* 2009;30(5):E603-E611.

38 Bu J, He S, Wang L, Li J, Liu J, Zhang X. A novel splice donor site mutation in EPHA2 caused congenital cataract in a Chinese family. *Indian J Ophthalmol* 2016;64(5):364-368.

39 Astiazarán MC, García-Montaño LA, Sánchez-Moreno F, Matiz-Moreno H, Zenteno JC. Next generation sequencing-based molecular diagnosis in familial congenital cataract expands the mutational spectrum in known congenital cataract genes. *Am J Med Genet A* 2018;176(12):2637-2645.

40 Reis LM, Tyler RC, Semina EV. Identification of a novel C-terminal extension mutation in EPHA2 in a family affected with congenital cataract. *Mol Vis* 2014;20:836-842.

41 Singh DR, Ahmed F, Paul MD, Gedam M, Pasquale EB, Hristova K. The SAM domain inhibits EphA2 interactions in the plasma membrane. *Biochim Biophys Acta BBA Mol Cell Res* 2017;1864(1):31-38.

42 Zhang L, Borthakur S, Buck M. Dissociation of a dynamic protein complex studied by all-atom molecular simulations. *Biophys J* 2016;110(4):877-886.

43 Park JE, Son AI, Hua R, Wang L, Zhang X, Zhou R. Human cataract mutations in EPHA2 SAM domain alter receptor stability and function. *PLoS One* 2012;7(5):e36564.

44 Ma X, Ma Z, Jiao X, Hejtmancik JF. Functional non-coding polymorphism in an EPHA2 promoter PAX2 binding site modifies expression and alters the MAPK and AKT pathways. *Sci Rep* 2017;7(1):9992.

45 Jun G, Guo H, Klein BEK, *et al*. EPHA2 is associated with age-related cortical cataract in mice and humans. *PLoS Genet* 2009;5(7):e1000584.

46 Dave A, Martin S, Kumar R, Craig JE, Burdon KP, Sharma S. EPHA2 mutations contribute to congenital cataract through diverse mechanisms. *Mol Vis* 2016;22:18-30.

47 Li Z, Quan Y, Gu S, Jiang JX. Beyond the channels: adhesion functions of aquaporin 0 and connexin 50 in lens development. *Front Cell Dev Biol* 2022;10:866980.

48 Cheng C, Gao J, Sun X, Mathias RT. Eph-ephrin signaling affects eye lens fiber cell intracellular voltage and membrane conductance. *Front Physiol* 2021;12:772276.

49 Parreno J, Emin G, Vu MP, Clark JT, Aryal S, Patel SD, Cheng C. Methodologies to unlock the molecular expression and cellular structure of ocular lens epithelial cells. *Front Cell Dev Biol* 2022;10:983178.

50 Vu MP, Cheng C. Mapping the universe of eph receptor and ephrin ligand transcripts in epithelial and fiber cells of the eye lens. *Cells* 2022;11(20):3291.

51 Murugan S, Cheng C. Roles of eph-ephrin signaling in the eye lens cataractogenesis, biomechanics, and homeostasis. *Front Cell Dev Biol* 2022;10:852236.

52 Zhang Y, Huang W. Transforming growth factor β1 (TGF-β1)-stimulated integrin-linked kinase (ILK) regulates migration and epithelial-mesenchymal transition (EMT) of human lens epithelial cells via nuclear factor κB (NF-κB). *Med Sci Monit* 2018;24:7424-7430.

53 Pontoriero GF, Smith AN, Miller LA, Radice GL, West-Mays JA, Lang RA. Co-operative roles for E-cadherin and N-cadherin during lens vesicle separation and lens epithelial cell survival. *Dev Biol* 2009;326(2):403-417.

54 Smith AN, Miller LA, Song N, Taketo MM, Lang RA. The duality of beta-catenin function: a requirement in lens morphogenesis and signaling suppression of lens fate in periocular ectoderm. *Dev Biol* 2005;285(2):477-489.